NATIONAL WATER RESEARCH INSTITUTE

INSTITUT NATIONAL de RECHERCHE sur les EAUX

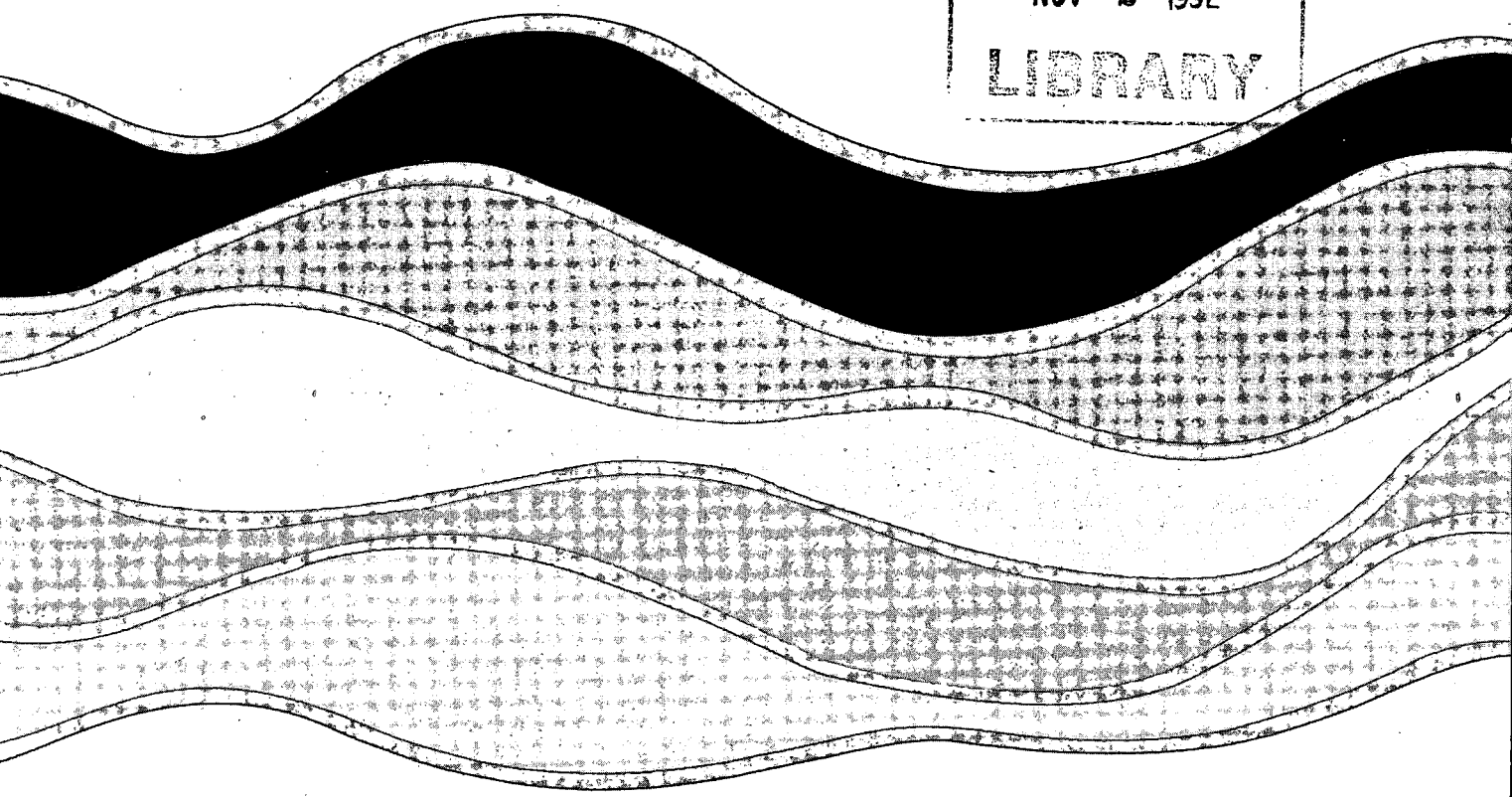

THE JOINT DISTRIBUTION OF HEIGHTS AND PERIODS OF SHOALING WAVES

J. C. Doering and M. A. Donelan

NWRI Contribution No. 92-16

THE JOINT DISTRIBUTION OF HEIGHTS AND PERIODS OF SHOALING WAVES

J. C. Doering[1]

and

M. A. Donelan

National Water Research Institute
Canada Centre for Inland Waters
Burlington, Ontario L7R 4A6

[1]Now at: Department of Civil Engineering
and Engineering Mechanics
McMaster University
Hamilton, Ontario L8S 4L7

August, 1992

MANAGEMENT PERSPECTIVE

Coastal engineering design practice depends heavily on theoretical and empirical models of the distribution of wave properties. Most emphasis has been placed on the distribution of heights of waves since there is a considerable body of theory and experience in this area. However, many design criteria hinge on the forces produced by the water flowing by coastal structures and structures moored in coastal waters. Estimates of these forces depend not only on the heights of waves but also on their periods. This work extends the body of knowledge of the joint distribution of heights and periods of waves from deep water right up to the breaker zone. The results and conclusions in this report give marine and coastal design engineers the material they need to improve both the economy and safety of their designs.

SOMMAIRE À L'INTENTION DE LA DIRECTION

La méthode de conception des travaux maritimes est fortement tributaire de modèles théoriques et empiriques de distribution des propriétés des vagues. On a mis l'accent principalement sur la distribution de la hauteur des vagues puisqu'il existe une masse de connaisances théoriques et beaucoup d'expérience dans ce domaine. Toutefois, de nombreux critères de conception dépendent des forces exercées par l'eau s'écoulant par des structures côtières et des structures mouillées dans les eaux côtières. L'estimation de ces forces est fonction non seulement de la hauteur des vagues, mais également de leur période. Ces travaux élargissent les connaissances de la distribution mixte de la hauteur et de la période des vagues depuis les eaux profondes jusqu'à la zone de déferlement. Les résultats et les conclusions du présent rapport fournissent aux ingénieurs responsables d'ouvrages de mécanique navale et d'ouvrages côtiers le matériel nécessaire pour rendre leurs conceptions plus économiques et plus sûrs.

ABSTRACT

The evolution of the joint distribution of wave heights and periods that results from shoaling is investigated using laboratory data obtained from experiments conducted on two (1:40 and 1:20) planar beach slopes. The data are compared to the theoretical joint distribution for wave heights and periods proposed by Longuet-Higgins (1983). For unbroken waves with $d/L > 0.1$ the shapes of the observed and predicted distributions agree reasonably well. However, the predicted joint distribution given by Longuet-Higgins (1983) is displaced relative to the observed distribution. A parametrization for the observed displacement is offered. In addition, a parametrization for variation of the spectral width parameter through the shoaling region is also given.

RÉSUMÉ

L'évolution de la répartition conjointe de la hauteur des vagues et de leur période lorsque soumises à la diminution de fond est étudiée au moyen de données de laboratoire obtenues à partir d'expériences effectuées sur deux plages planes à pentes de 1:40 et 1:20. Les données sont comparées à la distribution conjointe de la hauteur des vagues et de leur période telle qu'obtenue à partir de la theorie de Longuet-Higgins (1983). Dans le cas de vagues non déferlantes dont le rapport d/L est supérieur à 0,1, la forme des distributions observées et prévues concordent assez bien. Toutefois, la distribution conjointe prévue selon Longuet-Higgins (1983) est déplacée par rapport à la distribution observée. Une paramétrisation du déplacement observé est offerte. De plus, on fournit aussi une paramétrisation pour la variation de la largeur spectrale dans la région de diminution de fond.

1. INTRODUCTION

The joint distribution of wave heights and periods is of theoretical and practical interest to oceanographers and engineers. For example, it is required for the calculation of forces on structures. It can also be used to derive other joint distributions, such as the joint distribution of heights and slopes. Wave slope or steepness is, of course, related to wave breaking and the occurrence of whitecapping. This information is necessary for interpreting the backscatter power of microwave radars (Huang *et al.*, 1984) and for estimating the dissipation of wave energy and mixing of the upper ocean. The joint distribution of wave heights and periods can, of course, also be used to derive marginal distributions, for example, height, period, and steepness.

There is considerable engineering interest in the joint distribution of wave heights and periods as it is central to the design process. For example, it is important in the design of ocean platforms (Nolte, 1979) and coastal breakwaters (Losada and Giménez-Curto, 1979). It is also used in the design and testing of ships. The engineering significance of the joint distribution is not particularly surprising as it is well-known that the wave-induced forces on a structure arise from pressure, velocities, and accelerations, all of which are proportional to height and depend on the wave period.

The first approximation for the joint distribution of wave amplitudes and periods was proposed by Wooding (1955) who extended Rice's (1944, 1945) work on the distribution of intervals between successive zeros for a narrow spectrum of random noise. Longuet-Higgins (1957) independently proposed a similar formulation for the joint distribution of wave amplitudes and periods. This was work was subsequently distilled by Longuet-Higgins (1975) and applied to ocean waves. His formulation for the joint distribution defines a wave period as the time interval between successive zero-

up-crossings, and the corresponding wave height as the difference between the extrema (maximum and minimum) within the time interval. The distribution is applicable to a narrow spectrum of waves, *i.e.*, $\nu^2 \ll 1$, where ν is the spectral width parameter defined by the lowest three moments (μ_0, μ_1, and μ_2) of the variance density spectrum. However, this distribution has a symmetric wave period distribution that is not in keeping with observations (*e.g.*, Goda, 1978). Longuet-Higgins (1983) modified his distribution to include the asymmetry observed in the distribution of wave period.

Cavanié *et al.* (1976) developed a model for the joint distribution of wave heights and periods starting from the work of Cartwright and Longuet-Higgins (1956), at about the same time as Longuet-Higgins (1975). Their distribution, which accounts for the asymmetry observed in the wave period distribution, defines wave heights and periods using a wave crest-to-trough definition; that is, a wave period is defined by the time interval between successive crests while the corresponding wave height is given by the (vertical) difference between the crest and the succeeding trough. Like the joint distribution proposed by Longuet-Higgins (1983), the distribution given by Cavanié *et al.* (1976) is valid for narrow spectra and is uniquely defined by a spectral width parameter, in this case ε, which was defined by Cartwright and Longuet-Higgins (1956). However, unlike the spectral width parameter ν used by Longuet-Higgins (1975, 1983), ε depends on higher-order moments of the variance density spectrum, in particular, μ_4.

Longuet-Higgins assumes $\nu^2 \ll 1$ (an assumption used in the derivation of the joint distribution) to be satisfied when $\nu \leq 0.6$. For a fully-developed spectrum of deep water waves, the rear face has a slope of approximately f^{-4} (Donelan *et al.*, 1985). This yields a value for ν of ≈ 0.3 that is well below the "upper limit" of applicability assumed by Longuet-Higgins (1983). Moreover, since ν depends on relatively low-order moments of the variance density spectrum it converges relatively quickly. However, the spectral width parameter used by Cavanié *et al.* (1976) is a function of μ_0, μ_2, and μ_4.

If the rear face of a spectrum has an f^{-4} slope then μ_4 will not converge, instead it will increase monotonically. Its value becomes a direct function of the high frequency cut-off. Although ν is also somewhat dependent on the high frequency cut-off, it converges relatively quickly.

The "WAMP" (wave length and amplitude analysis) model developed by Lindgren (1972) and Lindgren and Rychlik (1982) has also been used to predict the joint distribution of heights (or amplitudes) and periods of waves. The model is based on properties of a normal process near a local maximum. The WAMP model differs from those of Cavanié *et al.* (1976) or Longuet-Higgins (1975, 1983), in that the results depend on the full covariance function of the time series and not only on a few spectral moments, such as those used to compute ϵ or ν. In particular, the WAMP model uses the covariance function and its first four derivatives to determine the wave length and amplitude distribution. Wave height and period in WAMP are both defined by a crest to succeeding trough approach; this definition for wave height is the same as that used by Cavanié *et al.* (1976), however, Lindgren's wave period is known as $T_{1/2}$, as it is defined by the time between a maximum and the succeeding minimum. The approximations used in the WAMP model are considered to be accurate for most narrow or moderate banded processes. Unfortunately, the WAMP model also depends on fourth-order quantities of the spectrum that are very sensitive to the high frequency cut-off (Srokosz and Challenor, 1987).

With the exception of the work by Srokosz and Challenor (1987), the studies that have compared deep water wave data to Longuet-Higgins joint distribution for wave heights and periods, where conducted prior to 1983, in particular, Chakrabarti and Cooley (1977), Goda (1978), and Shum and Melville (1984), and are therefore compared to Longuet-Higgins (1975) distribution. Perhaps surprising, is the reasonable agreement they found between the data and this joint distribution which did not

account for the asymmetric distribution of wave period. For $\nu \leq 0.4$ Srokosz and Challenor (1987) also noted reasonable agreement between their deep water data and the theoretical predictions given by Longuet-Higgins (1983).

Longuet-Higgins (1975) joint distribution for wave heights and periods was used by Le Méhauté *et al.* (1986) to theoretically examine the statistical properties of waves in intermediate depths of water. Le Méhauté *et al.* (1986) shoaled Longuet-Higgins' distribution using linear theory. They applied their theoretical formulation to a Pierson-Moskowitz spectrum for a fully-developed sea. Their results show that as shoaling begins there is a slight decrease in the probability of high wave heights which is followed by an increase in the probability of high wave heights as shoaling progresses further. This outcome is, of course, consistent with the intuitive expectation arising from linear theory. Their results were not compared to experimental data.

The applicability of joint distributions in the shoaling region (*i.e.*, intermediate and shallow water depths) has not been widely explored. Yet this information is clearly of practical importance. This is the purpose of the present paper. We concentrate here on Longuet-Higgins (1983) joint distribution since it is the only distribution that depends on a measurable spectral width parameter. A brief review of Longuet-Higgins (1983) joint distribution of wave heights and periods is outlined in the following section. The laboratory experiments that were undertaken for the present study are described in §3. The data reduction methodology is outlined in §4. The results of the data analysis are discussed in §5. A summary of the results is given in §6.

2. BACKGROUND

The joint distribution for wave heights and periods proposed by Longuet-Higgins (1983) is

$$p(H',T') = \frac{2}{\nu\sqrt{\pi}} \frac{H'^2}{T'^2} L(\nu) \exp\left\{-H'^2\left[1+\frac{\left(1-\frac{1}{T'}\right)^2}{\nu^2}\right]\right\},$$

where

$$L(\nu) = \frac{1}{\frac{1}{2}\left[1+\sqrt{1+\nu^2}\right]}$$

and

$$H' = \frac{H}{2\sqrt{2\mu_0}}, \quad T' = \frac{T}{\overline{T}}.$$

H' and T' are the normalized wave height and period, respectively, H is the wave height, T the period, and $\overline{T} = 2\pi\frac{\mu_0}{\mu_1}$, where the $^-$ denotes a mean value. The joint distribution is uniquely defined by the spectral width parameter ν, where

$$\nu = \sqrt{\frac{\mu_0\mu_2}{\mu_1^2} - 1}.$$

μ_0, μ_1, and μ_2 are moments of the variance spectrum. The n^{th} moment of the variance spectrum

$$\mu_n = \int_0^\infty f^n S(f) df,$$

where f is a frequency and S(f) is the corresponding density. The distribution is formally valid for $\nu^2 \ll 1$, which Longuet-Higgins assumes to hold for $\nu^2 \ll 0.36$.

3. THE LABORATORY EXPERIMENTS

The data used for this study were obtained from experiments conducted in the wind-wave flume at the National Water Research Institute. The flume is 103 m long, 4.5 m wide, and has a maximum water depth of 1.5 m. "Random" waves were generated using the GEDAP software package developed by the National Research

Table 1– Summary of Spectral Realizations

Run IDs	Type	U_c/c_p	f_p [Hz]	H_c [m]
GR30–33	DHH	0.83	0.9	0.06
GR34–37	DHH	5.00	0.9	0.11
GR02–05	DHH	0.83	0.8	0.08
GR06–09	DHH	5.00	0.8	0.14
GR10–13	DHH	0.83	0.7	0.10
GR14–17	DHH	5.00	0.7	0.19
GR18–21	DHH	0.83	0.6	0.14
GR22–25	DHH	5.00	0.6	0.25
GR26–29	DHH	0.83	0.5	0.20
GR39–42	DHH	0.83	0.4	0.32

Note:
U_c/c_p is the wave age parameter
f_p is the frequency of the spectral peak
H_c is the characteristic wave height defined here as $= 4\sqrt{\mu_0}$

Council of Canada (Funke and Mansard, 1984). Corrections were made to the piston-type waveboard drive signal to suppress spurious, second-order waves that arise through the mechanical generation of waves. All of the "random" wavetrains were created from DHH target spectra, after Donelan *et al.* (1985). The parameters of a DHH spectrum are similar to those of a JONSWAP spectrum, however, the DHH spectrum has an f^{-4} tail rather than the f^{-5} tail that is characteristic of a JONSWAP spectrum. Moreover, a DHH spectrum exhibits stronger peak enhancement at short fetches and greater directional spreading at high frequencies than a JONSWAP spectrum. Six peak frequencies (f_p=0.9, 0.8, 0.7, 0.6, 0.5, and 0.4 Hz) and two peak enhancement or wave age values (U_c/c_p=0.83 (fully developed) and 5.0 (strongly forced)) were used. Each run contained approximately 500 waves; four realizations of each spectral shape were run giving a total of over 2000 waves from which to construct the joint distribution of wave heights and periods. A summary of the runs is given in table 1. A water depth of 1.00 m was used for all runs.

The experiments were conducted on two impervious (plywood) beach slopes, 1:40 and 1:20. The toe of both beaches was located 27.7 m from the (mean position of the) waveboard; see figure 1. Wave heights (and periods) were measured using

surface-piercing capacitance-type wave probes. The electronics packages for the wave probes were designed and built by the technical support team at the National Water Research Institute. Wave probe calibration data shows that these instruments are very linear ($r^2 > 0.999$) and have excellent long term gain stability. Ten wave probes were installed on the 1:40 beach slope. The first wave probe was located at the toe of the beach, which was 27.7 m from the waveboard. The remaining nine wave probes were installed on 4 m centers; this yields a decrease in depth of 0.1 m between adjacent wave probes. For the 1:20 beach slope, fourteen wave probes were used. The first wave probe (WP 'A') was 7.7 m from the mean position of the waveboard, the next three synoptic probes (WPs 'B', 'C', and 'D') were installed on 5 m centers. The fifth wave probe (denoted WP 1), located at the toe of the 1:20 beach, was therefore 27.7 m from the waveboard; that is, in the same location and depth as WP 1 was on the 1:40 beach. The remaining nine probes were placed on 2 m centers; again, this yields a decrease of 0.1 m between adjacent probes. The intent was to position the ten wave probes (WP 1 to 10) on the 1:20 beach in the same depth of water as the respective wave probe was on the 1:40 beach.

Wave reflection from the beach was measured using a wave-wire array. The 1:40 beach yielded a reflection coefficient of approximately 4% for the longest peak period of 2.5 s waves, whereas a 7% reflection coefficient was obtained for the same period on the 1:20 beach. Shorter waves are, of course, reflected less, while longer period waves arising from radiation stress effects associated with wave groupiness are more strongly reflected.

Analog outputs (*i.e.*, wave probes) were lowpass filtered at 10 Hz then sampled digitally (with 12 bit resolution) at 20 Hz.

4. DATA REDUCTION

The wave heights and periods for each run were determined using a zero-up-crossing analysis. The procedure for computing the heights and periods from each time series was as follows. The mean water level was removed and zero-up-crossings identified (a negative elevation followed immediately by a zero or positive value). To eliminate the 20 Hz (50 ms) sampling quantization error, the time of each zero-up-crossing was estimated using a linear interpolation. With peak periods ranging from 1.11 to 2.5 s, the error associated with linear interpolating the zero-up-crossing of 20 Hz data is very small. Higher-order interpolation (quadratic) was investigated, however, it yielded virtually identical results while adding considerably to the computational requirements; for this reason, linear interpolation was used. Wave period was defined as the time interval between successive zero-up-crossings.

The corresponding wave height was computed from the difference between the maximum and minimum located between the zero-up-crossings. This yields computed wave heights that are slightly smaller than the "true" wave height because it is unlikely that sampling will occur exactly on the extrema (maximum and minimum). However, in light of the sampling rate to wave period ratios, the error introduced is believed to be quite small. Moreover, one could introduce even larger errors by employing some *ad hoc* method of interpolating, such as extrapolating slopes or nonlinear fitting of the last n points on either side of the extrema.

To generate the plots of the joint distribution of wave heights and periods, the data were binned and contoured. All of the aforementioned data analysis was performed using MATLAB software (Little and Moler, 1990).

5. DATA ANALYSIS & DISCUSSION

The model of Longuet-Higgins (1983) was chosen for comparison to the data because it is relatively insensitive to the high frequency cut-off compared to the models of Lindgren (1972) and Cavanié *et al.* (1976). The models of Lindgren (1972) and Cavanié *et al.* (1976) define wave height as the vertical distance between the crest and preceding trough. Even relatively small high-frequency waves superimposed on the dominant or peak wave period will therefore be defined as a wave. This tends to produce a joint distribution for wave heights and periods whose contours are (not predictably) crowded against the origin because these high frequency waves are relatively numerous. The existence and structure of these waves is critically linked to the high frequency content and cut-off of the spectrum, thus so is the observed joint distribution. However, the zero-up-crossing definition for a wave, which Longuet-Higgins (1983) used, avoids this problem. Longuet-Higgins (1983) distribution is therefore relatively insensitive to the high frequency content and cut-off while the joint distributions due to Lindgren (1972) and Cavanié *et al.* (1976) are critically dependent on it. During preliminary studies it was determined that it was necessary to filter the time series (before computing the wave heights and periods) to obtain joint distributions that were similar to those predicted by Lindgren (1972) and Cavanié *et al.* (1976). The arbitrariness of choice of the filter characteristics made it difficult to apply these distributions consistently, thus, these distributions were not considered further.

As indicated in table 1, ten different spectral shapes where shoaled over both the 1:40 and 1:20 beach slopes. Although all of the data were considered during the analysis, the presentation of data will be limited here to two runs, GR18-21 and GR22-25. Run GR18-21 is a fully-developed ($U_c/c_p = 0.83$) spectrum of waves with a peak frequency, f_p, of 0.6 Hz, whereas run GR22-25 is a strongly-forced ($U_c/c_p = 5.00$) spectrum with peak frequency of 0.6 Hz also. These two runs were selected because

both of them nicely illustrate the evolution of the joint distribution of wave heights and periods that arises from shoaling while contrasting the differences between a fully-developed versus a strongly-forced spectrum. Results from both beaches are presented.

The variation of μ_0, μ_1, and μ_2 as a function of f/f_p for a fully-developed DHH spectrum with $f_p = 0.6$ Hz is shown in figure 2(a); f denotes the upper limit of integration used in the computation of the spectral moments. μ_0 and μ_1 rapidly converge by $f/f_p \approx 3$, whereas μ_2 is slightly slower to converge. The relatively rapid convergence of μ_0 and μ_1 by $f/f_p \approx 3$ yields stable estimates of $H_{rms} = 2\sqrt{2\mu_0}$ and $\overline{T} = 2\pi\mu_0/\mu_1$, which are used to normalize the wave heights and periods, respectively. Although the spectral moments used to compute ν are not as sensitive to the cut-off frequency as those involving higher-order moments, a cut-off frequency must nonetheless be chosen; moreover, it should be consistently defined. As such ν was computed using frequencies from $\frac{1}{2}f_p \rightarrow 3.0f_p$, which is the band containing approximately 99% of the integrated spectral variance. The lower limit was imposed to avoid the small contribution from longwaves, which have a variable spatial contribution and thus impose a small unpredictable "jitter" in the value of ν. Figure 2(b) shows the variation of ν as a function of f/f_p.

A short segment of surface elevation from run GR18-21 ($U_c/c_p = 0.83$, $f_p = 0.6$ Hz) over the 1:40 beach is shown in figure 3(a). Note, the records have been shifted for plotting purposes. The wave probe number (WP No.), water depth (d), d/L ratio, spectral width (ν), standard deviation ($\sqrt{\mu_o}$), normalized skewness (S_N), and Ursell parameter (Ur), for these data are summarized in table 2. The Ursell parameter is used here as a measure of the strength of shallow water nonlinearities. It is formally defined as (Ursell, 1953)

$$Ur = \frac{3}{4}\frac{ak}{(kd)^3},$$

where a is an amplitude, k is the radian wavenumber, and d is the water depth. The

Table 2– Summary of Parameters for Runs GR18-21 & GR22-25

Run	Beach	WP No.	d [m]	d/L	ν	$\sqrt{\mu_0}$	S_N	Ur
GR18-21	1:40	1	0.943	0.24	0.30	0.0357	0.19	0.0095
		4	0.628	0.18	0.30	0.0348	0.32	0.0268
		7	0.341	0.12	0.36	0.0334	0.54	0.1099
		9	0.140	0.07	0.42	0.0229	1.16	0.4662
GR18-21	1:20	1	0.944	0.24	0.30	0.0365	0.22	0.0087
		4	0.661	0.19	0.31	0.0358	0.31	0.0224
		7	0.357	0.13	0.35	0.0355	0.57	0.0978
		9	0.162	0.08	0.42	0.0315	0.95	0.4658
GR22-25	1:20	1	0.944	0.24	0.25	0.0579	0.27	0.0205
		4	0.661	0.19	0.28	0.0564	0.49	0.0501
		7	0.357	0.13	0.37	0.0533	0.76	0.1962
		9	0.162	0.08	0.42	0.0348	0.84	0.6475

waves observed at WP 1 (figure 3(a), top record), $d/L = 0.24$, are nearly symmetric with respect to mean water level shown by the dashed line, *i.e.*, the record has a relatively small skewness ($S_N = 0.19$). However, in shallower depths ($d/L = 0.18$, 0.12, and 0.07) there is a pronounced peaking of the wave crests and elongation of the troughs. This is reflected in the increased skewness of the records (see table 2). A distinct increase in the vertical asymmetry of the waves can also be observed. These characteristics readily indicate the existence of strong nonlinear interactions associated with shoaling. The region of breaking for this run was roughly centered around WP 8. Thus WPs 1, 4, and 7, (the top three records) were outside the region of breaking, while WP 9 (the bottom record) was located inside the surf zone. The loss of energy associated with wave breaking can be readily observed in the standard deviations ($\sqrt{\mu_0}$) listed in table 2. These standard deviations can, of course, be used to compute characteristic wave heights, defined here as $H_c = 4\sqrt{\mu_0}$, which yields characteristic heights of 14.3, 13.9, 13.3, and 9.2 cm, for WPs 1, 4, 7, and 9, respectively.

The spectra corresponding to the four time series shown in figure 3(a) are given in figure 3(b). The spectra from WPs 1, 4, and 7 are essentially coincident with the exception of the low frequency energy. The near coincidence is anticipated since the standard deviations of these records are very similar. The spectrum for WP 9, on

the other hand, lies below those for the deeper probes but has a smaller (less steep) tail slope. The net result is a marked reduction in variance brought about by wave breaking. The variation in the low frequency energy observed in figure 3(b) is probably due to the spatial dependence of quasi-standing long-waves that arise from radiation stress effects associated with wave groupiness. These waves are unlikely to be unwanted artifacts of the wave generation process as an effective spurious long wave suppression algorithm was incorporated into the wave generation process.

Figures 3(c)-3(f) show the evolution of the joint distribution of wave heights and periods associated with shoaling for run GR18-21. Recall, $U_c/c_p = 0.83$ and $f_p = 0.6$ Hz, for these data. At the toe of beach (WP 1, $d/L = 0.24$, figure 3(c)) there is good agreement between the observed and predicted distributions, indicating that Longuet-Higgins (1983) can provide reasonable predictions of the joint distribution in intermediate water depths (*i.e.*, $0.05 < d/L < 0.5$). In shallower water depths, $d/L = 0.018$ and 0.12, figures 3(d) and 3(e), respectively, good agreement is also observed between the predicted and observed shapes of the joint distributions. However, after breaking ($d/L = 0.07$), figure 3(f), the joint distribution is not well predicted. Wave breaking and reformation have significantly altered the shape of the joint distribution. In particular, there is an increase in the density or probability of relatively high wave heights with long periods (upper righthand corner).

The dashed line shown in figures 3(c)-3(e) is the finite depth wave steepness limit given by Miche (1944),

$$\left(\frac{H}{L}\right)_{max} = 0.142 \tanh\left(\frac{2\pi d}{L}\right),$$

where d and L are the local still water depth and wavelength, respectively. For all of the unbroken wave cases, figures 3(c)-(e), the Miche limit defines the left hand edge of the distribution. This is particularly intriguing as Longuet-Higgins (1983) joint distribution is simply a mathematical model for random noise and embodies no wave

physics. The Miche limit is not shown for the shallowest station as the limit is not expected to hold for such highly nonlinear waves.

Figure 4 shows the results for run GR18-21 on the 1:20 beach slope. The similarity to figure 3, run GR18-21 on the 1:40 beach slope, is readily evident. A comparison of figures 3(a) and 4(a) indicates that the surface displacements at the toe of both beaches were nearly identical; small differences are expected to arise from effects associated with the different beach slopes. At shallower water depths, *i.e.*, WPs 4 and 7, a reasonable correlation is observed between the record from the 1:40 beach and that from the 1:20 beach. This finding is consistent with Stive (1980) who noted, "From the surface variations it can be concluded that the water motion at each depth seems to be strongly locally controlled". Again, small differences are not unexpected as the evolution distance on the 1:40 beach is twice that of the 1:20 beach slope (4 m between wave probes versus 2 m, respectively). Moreover, for a given wave probe there is a small difference in the still water depths between the two beaches arising from installation errors and plywood "beach" warpage (see table 2). An inspection of the parameters summarized in table 2 further indicates the similarity of the data from WP 1, 4, and 7, over the 1:40 and 1:20 beach slopes. However, after breaking (WP 9) a correlation is not readily evident. Differences between WP 9 data for the two beaches are also readily apparent in the measured standard deviation and skewness.

The spectra shown in figure 4(b) are similar to those in figure 3(b) for frequencies above $1/2 f_p = 0.3$ Hz. Below 0.3 Hz, however, there are some distinct differences which probably arise from the (different) spatial structure of the low frequency energy over the 1:40 and 1:20 beach slopes. It is unlikely that the differences arise from varying reflection characteristics of the two beaches, as low frequencies such as these would probably have very similar reflection coefficients (Tatavarti, 1989).

The evolution of the joint distributions of wave heights and periods observed at wave probes 1, 4, and 7 are remarkably similar for both beaches. The predicted distributions are, for all practical purposes, identical as the spectral width parameters are roughly equal for a given depth on the 1:40 beach slope to that on the 1:20 beach slope. However, after breaking there is a significant difference between the two joint distributions observed on the 1:40 beach slope and on the 1:20 beach slope. In particular, the modal value of the joint distribution for the 1:20 beach slope lies further from the origin than that for the 1:40 beach.

Figure 5 shows the results from the 1:20 beach for run GR22-25, which is a strongly-forced spectrum of waves with a peak frequency of 0.6 Hz. As for the fully-developed case, the waves initially have small skewness and small vertical asymmetry (figure 5(a), WP 1; also see table 2) but become highly skewed and vertically asymmetric or steep faced (WPs 7 and 9) in shallow water as a result of the strong nonlinearities associated with shoaling. The strongly-forced nature of these waves can be seen in the short segments of time series and the spectra. The characteristic wave height at WP 1 for run GR22-25 is almost 60% larger than that observed at the same wave probe for run GR18-21; 23.2 cm versus 14.6 cm, respectively. The spectra in figure 5(b) are clearly peakier and more energetic than those shown in figure 4(b). The peakier and thus narrower spectra yield a smaller spectral width parameter, ν. Figures 5(c)-(f) show the observed and predicted joint distributions of wave heights and periods for run GR22-25. Inspection of figures 5(c) and 5(d) readily indicates that these joint distributions are narrower than those observed for the fully-developed run GR18-21 shown in figures 3(c)-(d) and 4(c)-(d). The agreement between the observed and predicted distributions at wave probes 1 and 4 is reasonable; figures 5(c) and 5(d), respectively. However, at WP 7 where active breaking has already begun the agreement diminishes. The strongly-forced nature of run GR22-25 produces taller, steeper waves that are modified by nonlinearities and limited by finite depth effects sooner than those of run

GR18-21. The shape of the joint distribution observed inside the surf zone for this run, is similar to that for run GR18-21 on the 1:40 and 1:20 beach slopes.

The observations of the joint distributions shown in figures 3, 4, and 5, indicate that although the observed and predicted joint distributions outside the active region of wave breaking are very similar, they are not coincident, that is, they appear to be slightly displaced; this can be readily observed in figures 3(c-e), 4(c-e), and 5(c-d). To estimate the displacement between the observed and predicted distributions the rms error was considered. By shifting the predicted joint distribution slightly it was found that the rms error between the observed and predicted joint distributions could be minimized. Figure 6(a) shows the variation of C_H, the parameter used to shift the predicted distribution along the normalized wave height axis H', as a function of ν for all ten runs. Similarly, the factor C_T, which was used to shift the predicted distribution along the normalized wave period axis T', as a function of ν is shown in figure 6(b). The 'o' symbols indicate unbroken waves while the '+' symbols denote broken wave data. The parameter C_H is correlated with ν, whereas C_T is not well correlated with ν. The least-squares regression lines shown were fit using only the unbroken wave data. There is little point in using the broken wave data as the shape of the predicted joint distribution is significantly different than that observed for broken waves (*e.g.*, figures 3(f), 4(f), 5(e) and 5(f)). Figure 6(a) and 6(b) indicate that, in general, the predicted joint distribution needs to be shifted down (C_H typically < 1) and to the right (C_T typically > 1) to minimize the error between the observed and predicted distributions. This result is, of course, heavily weighted by the large probabilities around the modal value and suggest that the modal value is not exactly predicted by Longuet-Higgins (1983). A similar observation was noted by Srokosz and Challenor (1987).

The joint distribution given by Longuet-Higgins (1983) is uniquely defined by one parameter, the spectral width, ν. The prediction of ν through the shoaling

region is therefore of interest. Figure 7 shows the variation of ν as a function of the Ursell parameter. The Ursell parameter can be interpreted physically as the ratio of wave steepness (ak) to relative depth (kd). The '+' symbols denote the fully-developed spectral runs, whereas the '$*$' symbols indicate the strongly-forced runs. The correlation in both cases is quite good. The equations for the second-order least squares fit presented are as follows:

1. fully-developed ($U_c/c_p = 0.83$)

$$\nu = 0.28, \quad Ur \leq 0.0018$$

$$\nu = 0.46 + 0.058\ln(Ur) + 0.0046[\ln(Ur)]^2, \quad Ur > 0.0018$$

2. strongly-forced ($U_c/c_p = 5.00$)

$$\nu = 0.23, \quad Ur \leq 0.0049$$

$$\nu = 0.51 + 0.11\ln(Ur) + 0.0099[\ln(Ur)]^2, \quad Ur > 0.0049$$

Wave ages (U_c/c_p) other than those considered would presumably lie within the two extremes of 0.83 and 5.00 that were considered.

Since the Ursell parameter can be readily modeled through the shoaling region (Doering, 1988), this provides a simple predictive scheme for ν and thus for the joint distribution of wave heights and periods as given by Longuet-Higgins (1983). Inside the surf zone the distribution changes shape markedly to one where the correlation between heights and periods is pronounced (Thornton and Schaeffer, 1978). The waves in the surf zone are highly nonlinear and the assumption of Gaussianity inherent in the development of Longuet-Higgins (1983) clearly do not apply.

Finally, it is worth mentioning that an alternative to using ν to predict the joint distribution of wave heights and periods of shoaling waves is to use linear theory to

shoal the joint distribution. Figure 8 shows the results of shoaling the joint distribution for run GR18-21 on the 1:40 beach slope. Comparison of figures 3(c-e) and 8(a-c), respectively, indicates that linearly shoaling the joint distribution does not provide as good a fit to the data as parameterizing the change in ν that results from shoaling. The shoaled distributions for WPs 1, 4, and 7 underpredict the occurrence of high waves (figures 8(a-c), respectively). Close inspection of figures 8(a-c) also indicates that there is a slight decrease in the probability of long wave periods expected, yet the data suggests that there is an increase in the occurrence of long waves. This increase in the probability of long waves is predicted by the increasing magnitude of ν associated with shoaling (figures 3(c-e)). The joint distribution of broken waves (WP 9, figures 3(f) and 8(d)) is not well predicted by either method.

6. CONCLUSIONS

The evolution of the joint distribution of wave height and period was investigated using laboratory data collected on 1:40 and 1:20 planar beach slopes. These data were compared to the joint distribution for wave heights and periods proposed by Longuet-Higgins (1983). This distribution was selected for comparison because it is not as sensitive to the choice of the high frequency spectral cut-off as other models. The comparison between the data and Longuet-Higgins (1983) joint distribution indicates that it provides a reasonable fit to unbroken waves provided $d/L > 0.1$, which is close to the shallow limit of $d/L < 0.05$. However, after wave breaking ensues the observed joint distribution differs significantly from the shape predicted by Longuet-Higgins (1983). The observations indicate that although the shape of the joint distribution is reasonably well predicted by Longuet-Higgins (1983), it is not coincident with the observed distribution, instead it is shifted slightly. The shift of the predicted distribution was shown to be weakly correlated with the spectral width parameter ν which is the sole parameter used to define the predicted distribution. Moreover, ν was found to be

strongly correlated with the Ursell parameter, Ur. The parametrization of ν is of considerable practical importance because it provides a simple method for the predicting the joint distribution of wave heights and periods in the shoaling region.

ACKNOWLEDGMENTS

This research was conducted while the first author was a postdoctoral fellow at the National Water Research Institute, Canada Centre for Inland Waters, Burlington, Ontario. The superb hospitality and generous support that were provided during that time are very gratefully acknowledged. The technical support provided by B. Taylor, G. Voros, K. Davis, and T. Nudds for the laboratory experiments was greatly appreciated. This study was lead by Dr. M. Skafel. Funding was provided by the Panel for Energy Research and Development (PERD), task 6.2, study 62124.

REFERENCES

Cartwright, D.E. and M.S. Longuet-Higgins, 1956. The statistical distribution of the maxima of a random function. *Proc. Roy. Soc.*, **A237**, 212–232.

Cavanié, A., M. Arhan, and R. Ezraty, 1976. A statistical relationship between individual heights and periods of storm waves. *Proc. of Behaviour of Offshore Structures*, Trondheim, 354–360.

Chakrabarti, S.K., and R.P. Cooley, 1977. Statistical distribution of periods and heights of ocean waves. *J. Geophys. Res.*, **82-9**, 1363–1368.

Doering, J.C., 1988. Wave-wave interactions in the nearshore. Ph.D. Thesis, Dalhousie University, Halifax, 139 p.

Donelan, M.A., J. Hamilton, and W.H. Hui, 1985. Directional spectra of wind-generated waves. *Phil Trans. R. Soc. Lond.*, **A315**, 509–562.

Funke, E.R., and E.P.D. Mansard, 1984. The NRCC "random" wave generation package. *Tech. Report NRC*, Ottawa, no. 23571, TR-HY-002, 78 p.

Goda, Y., 1978. The observed joint distribution of periods and heights of sea waves. *Proc. 16th Int. Conf. on Coastal Eng.*, Sydney, Australia, 227–246.

Huang, N.E., S.R. Long, L.F. Bliven, and C. Tung, 1984. The Non-Gaussian joint probability density function of slope and elevation for a nonlinear gravity wave field. *J. Geophys. Res.*, **89-C2**, 1961–1972.

Le Méhauté, B., C.C. Lu, and E.W. Ulmer, 1986. Proceedings of the 1981 conference on Wave Dynamics and Radio Probing of the Ocean Surface, O.M. Phillips and K. Hasselmann (editors), 181–191

Lindgren, G., 1972. Wave-length and amplitude in Gaussian noise. *Adv. Appl. Prob.*, **4**, 81–108.

Lindgren, G., and I. Rychlik, 1982. Wave characteristic distributions for Gaussian waves – Wave-length, amplitude, and steepness. *Ocean Engng.*, **9**, 411–432.

Little, J., and C. Moler, 1990. MATLAB for 80386-based MS-DOS personal computers, User's Guide. The Math Works Inc.

Longuet-Higgins, M.S., 1957. The statistical analysis of a random, moving surface. *Phil. Trans. Roy. Soc. London*, **A249**, 321–387.

Longuet-Higgins, M.S., 1975. On the joint distribution of the periods and amplitudes of sea waves. *J. Geophys. Res.*, **80-18**, 2688–2694.

Longuet-Higgins, M.S., 1983. On the joint distribution of wave periods and amplitudes in a random wave field. *Proc. R. Soc. London*, **A389**, 241–258.

Losada, M.A., and L.A. Giménez-Curto, 1979. The joint effect of wave height and period on the stability of rubble- mound breakwaters using Iribarren's number. *Coastal Eng.*, **3**, 77–96.

Miche, R., 1944. Mouvements Ondulatoires de la Mer en Profondeur Constante ou Decroissante. *Annales de Ponts et Chaussees.*

Nolte, K.G., 1979. Joint probability of wave period and height. *J. of the Waterway, Port, Coastal, and Ocean Division*, ASCE, **105-WW4**, 470–474.

Shum, K.T., and W.K. Melville, 1984. Estimates of the joint statistics of amplitudes and periods of ocean waves using an integral transform technique. *J. Geophys. Res.*, **89-C4**, 6467–6476.

Srokosz, M.A., and P.G. Challenor, 1987. Joint distributions of wave height and period: a critical comparison. *Ocean Engng.*, **14-4**, 295–311.

Stive, M.J.F., 1980. Velocity and pressure field of spilling breakers. *Proc. of the* 17^{th} *Conf. on Coastal Eng.*, ASCE, 547–566.

Tatavarti, V.S.N., 1989. The reflection of waves on natural beaches. *Ph.D. Thesis*, Dalhousie University, Halifax, N.S., pp. 175.

Thornton, E.B., and G. Schaeffer, 1978. Probability density functions of breaking waves. *Proc. of the* 16^{th} *Conf. on Coastal Eng.*, ASCE, 507–519

Rice, S.O., 1944. The mathematical analysis of random noise. *Bell Syst. Tech. J.*, **23**, 282–332.

Rice, S.O., 1945. The mathematical analysis of random noise. *Bell Syst. Tech. J.*, **24**, 46–156.

Ursell, F., 1953. The long-wave paradox in the theory of gravity waves. *Proc. Cambridge Philos. Soc.*, **49**, 685–694.

Wooding, R.A., 1955. An approximate joint probability distribution for amplitude and frequency in random noise. *N.Z.J. Sci. Tech.*, **B36**, 537–544.

LIST OF SYMBOLS

Symbol	Designation
a	amplitude
c_p	phase speed of the spectral peak
C_H	wave height optimization factor
C_T	wave period optimization factor
d	still water depth
f	frequency
f_p	peak spectral frequency
g	acceleration due to gravity
H	wave height
H'	normalized wave height ($= H/H_{rms}$)
H_c	characteristic wave height ($= 4\sqrt{\mu_0}$)
H_{rms}	rms wave height ($= 2\sqrt{2\mu_0}$)
k	radian wavenumber ($= 2\pi/L$)
L	wave length
n	subscript
$p(H', T')$	probability of joint height and period occurrence
p_{max}	maximum probability
S_N	normalized (dimensionless) skewness
$S(f)$	spectral density
T	wave period
T'	normalized wave period ($= T/(\mu_0/\mu_1)$)
T_p	peak wave period
$\overline{T}$	mean wave period
U_c	wind speed
Ur	Ursell parameter ($= (ak)/(kd)^3$)
μ_n	n^{th} spectral moment
ν	spectral width parameter
ε	spectral width parameter

LIST OF FIGURES

Figure 1. Cross-section of 1:10 scale experimental arrangements used for the 1:40 and 1:20 beach slopes.

Figure 2. **(a)** Variation of μ_0, μ_1, and μ_2 as a function of f/f_p. Computation was performed using a fully-developed ($U_c/c_p = 0.83$) DHH spectrum of waves with $f_p = 0.6$ Hz. **(b)** Corresponding variation of ν as a function of f/f_p for the moments shown in (a).

Figure 3. **(a)** Short segment of the surface displacement time series recorded from wave probes 1 (top), 4, 7, and 9 (bottom) on the 1:40 beach slope. The still water depths are 0.943, 0.628, 0.341, and 0.140 m, respectively. Note, the traces have been separated for plotting purposes. The dashed line indicates the still water level. **(b)** Spectra corresponding to the four surface displacement records shown in (a); — WP 1, - - - WP 4, ··· WP 7, and - · - · WP9. There are 100 d.o.f. A fully-developed ($U_c/c_p = 0.83$) DHH target spectrum with $T_p = 1.67$ s, was used. **(c-f)** Contours of the joint distribution of wave heights and periods for WP 1, 4, 7, and 9, respectively. The dotted contours show the theoretical expectation from Longuet-Higgins (1983). Contours are shown for $(0.1, 0.3, 0.5, 0.7, 0.9, 0.99) \times p_{max}$.

Figure 4. **(a)** Short segment of the surface displacement time series recorded from wave probes 1 (top), 4, 7, and 9 (bottom) on the 1:20 beach slope. The still water depths are 0.944, 0.661, 0.357, and 0.161 m, respectively. Note, the traces have been separated for plotting purposes. The dashed line indicates the still water level. **(b)** Spectra corresponding to the four surface displacement records shown in (a); — WP 1, - - - WP 4, ··· WP 7, and - · - · WP9. There are 100 d.o.f. A fully-developed ($U_c/c_p = 0.83$) DHH target spectrum with $T_p = 1.67$ s, was used. **(c-f)** Contours of the joint distribution of wave heights and periods for WP 1, 4, 7, and 9, respectively. The dotted contours show the theoretical expectation from Longuet-Higgins (1983). Contours are shown for $(0.1, 0.3, 0.5, 0.7, 0.9, 0.99) \times p_{max}$.

Figure 5. **(a)** Short segment of the surface displacement time series recorded from wave probes 1 (top), 4, 7, and 9 (bottom) on the 1:20 beach slope. The still water depths are 0.944, 0.661, 0.357, and 0.161 m, respectively. Note, the traces have been separated for plotting purposes. The dashed line indicates the still water level. **(b)** Spectra corresponding to the four surface displacement records shown in (a); — WP 1, - - - WP 4, ··· WP 7, and - · - · WP9. There are 100 d.o.f. A strongly-forced ($U_c/c_p = 5.00$) DHH target spectrum with $T_p = 1.67$ s, was used. **(c-f)** Contours of the joint distribution of wave heights

and periods for WP 1, 4, 7, and 9, respectively. The dotted contours show the theoretical expectation from Longuet-Higgins (1983). Contours are shown for $(0.1, 0.3, 0.5, 0.7, 0.9, 0.99) \times p_{max}$.

Figure 6. **(a)** Coefficient applied to the normalizing wave height (H') of the predicted joint distribution, to minimize the total mean squared error between the predicted and observed joint distributions, expressed as a function of ν. **(b)** Coefficient applied to the normalizing wave period (T') of the predicted joint distribution, to minimize the total mean squared error between the predicted and observed joint distributions, expressed as a function of ν.

Figure 7. Spectral width parameter ν as a function of the Ursell parameter Ur for fully-developed (+) and strongly-forced (*) shoaling spectra. The solid and dashed lines indicate the least squares quadratic fit for the fully-developed and strongly-forced cases, respectively.

Figure 8. **(a-d)** Contours of the joint distribution of wave heights and periods for WP 1, 4, 7, and 9, respectively. The dotted contours show the theoretical expectation given by linearly shoaling Longuet-Higgins (1983). Contours are shown for $(0.1, 0.3, 0.5, 0.7, 0.9, 0.99) \times p_{max}$.

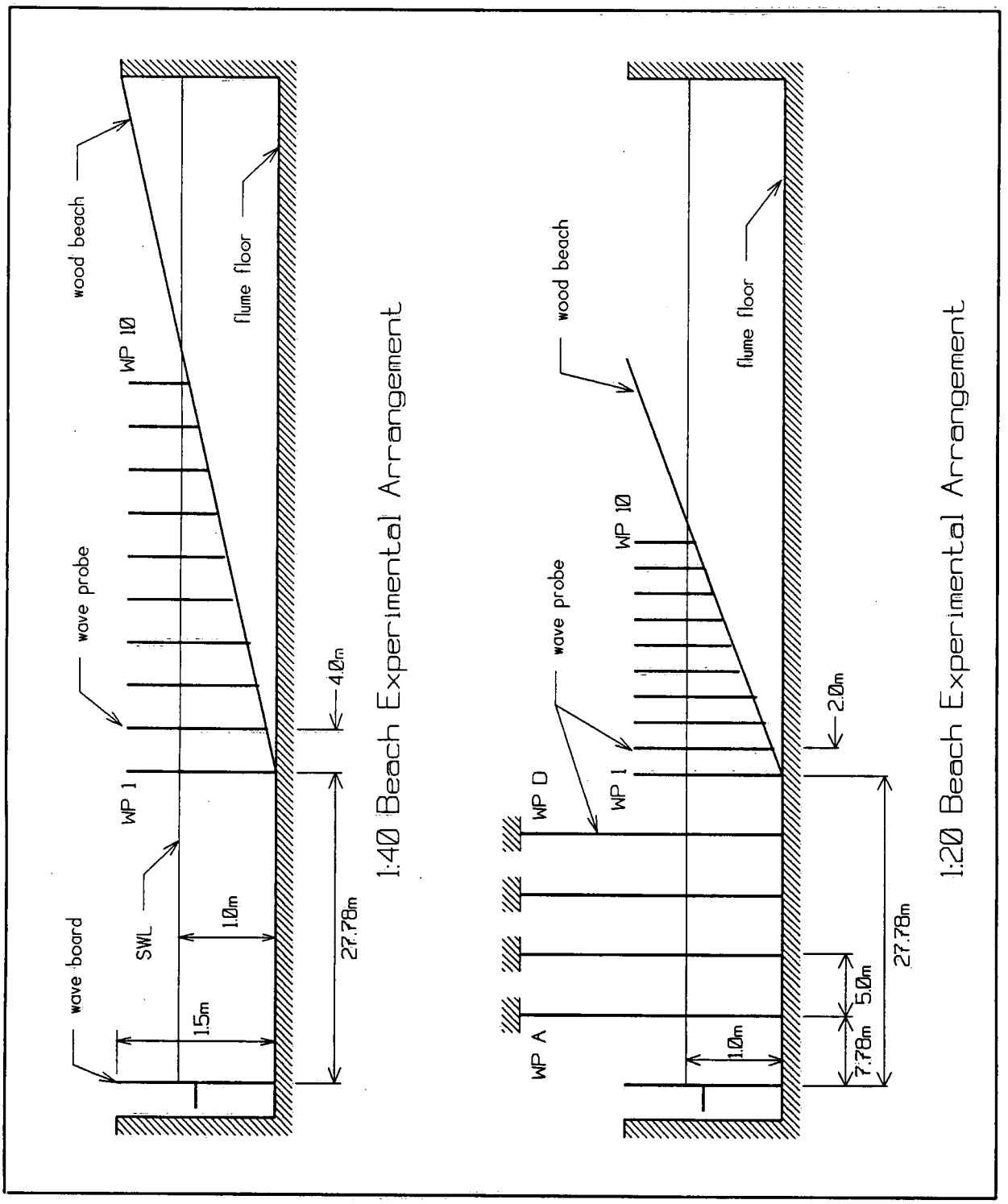
wood beach
flume floor
WP 10
wave probe
WP 1
SWL
wave board
1.0m
1.5m
27.78m
4.0m
1:40 Beach Experimental Arrangement
wood beach
flume floor
WP 10
wave probe
WP 1
WP D
WP A
2.0m
1.0m
7.78m
5.0m
27.78m
1:20 Beach Experimental Arrangement

Figure 1

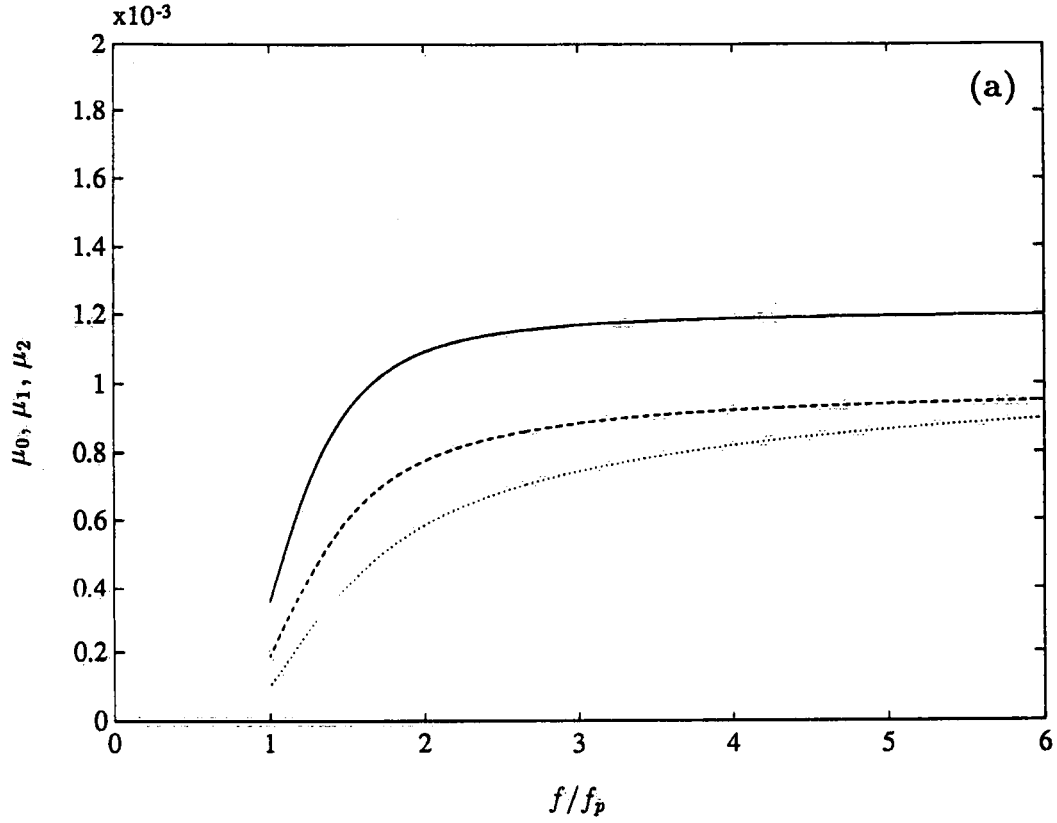

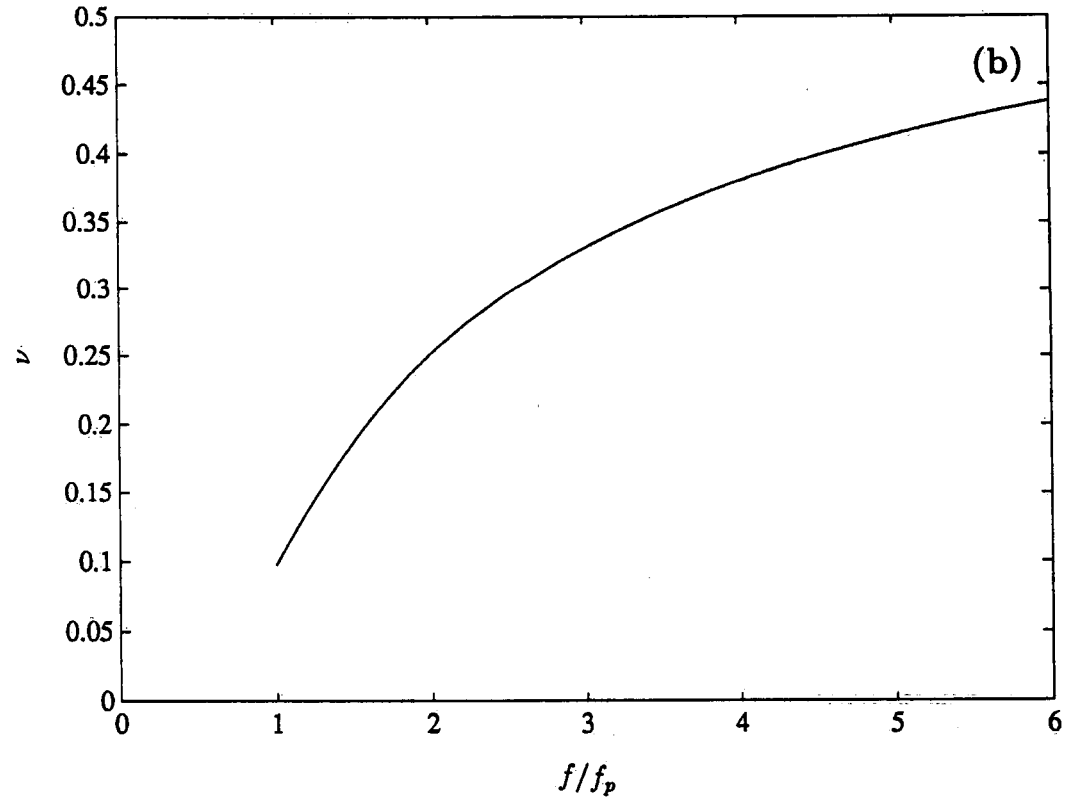

Figure 2

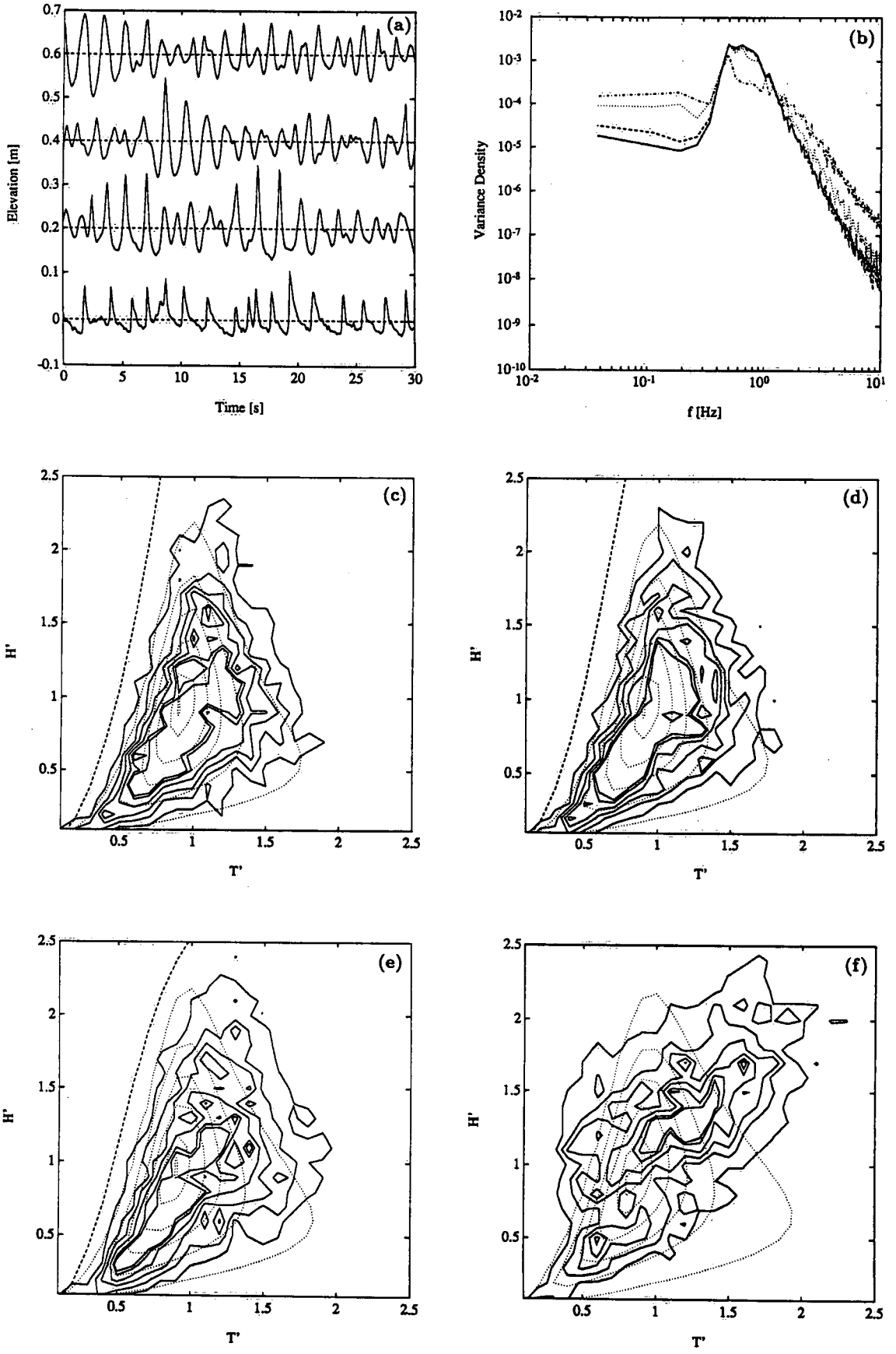

Figure 3

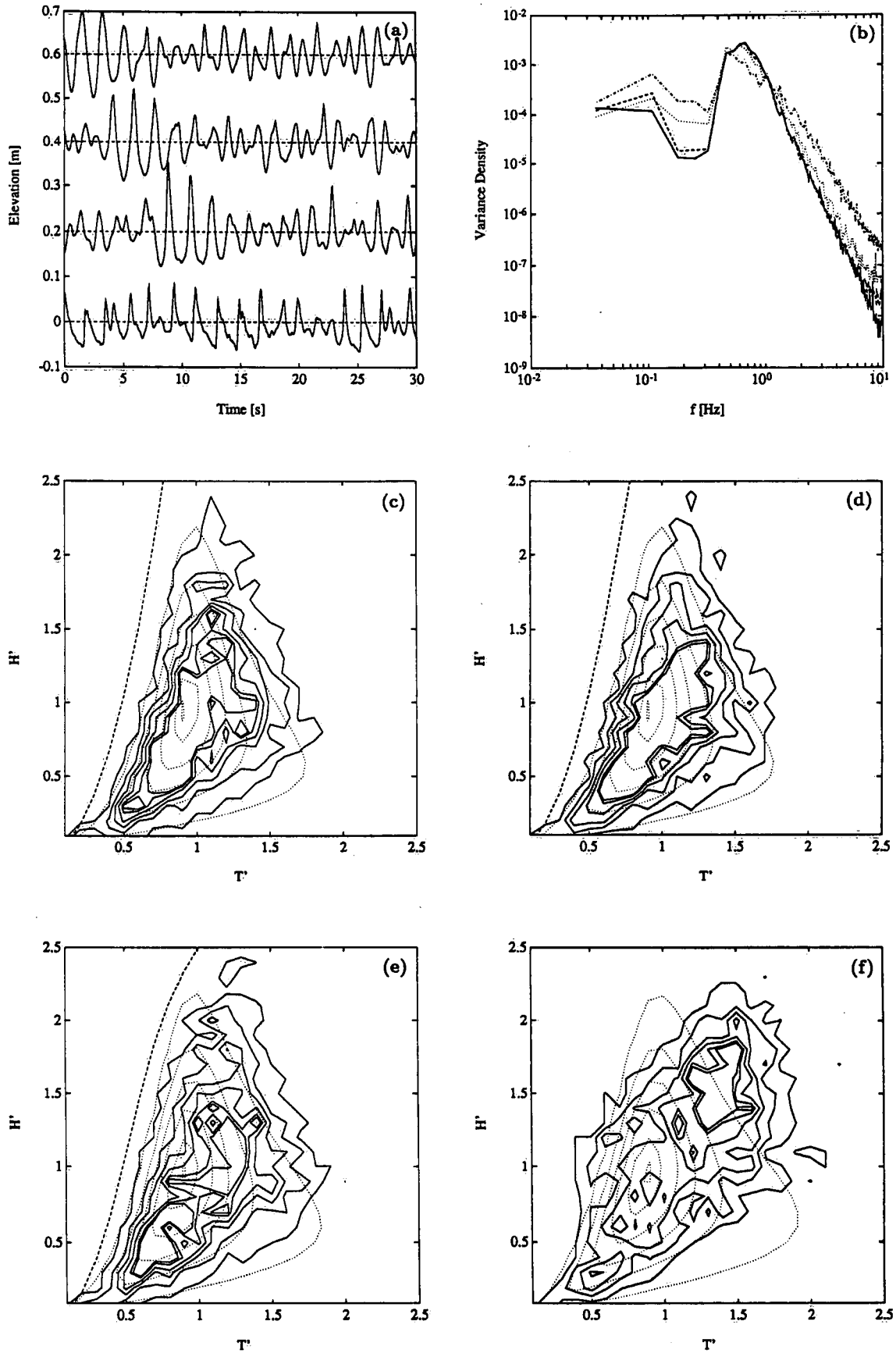

Figure 4

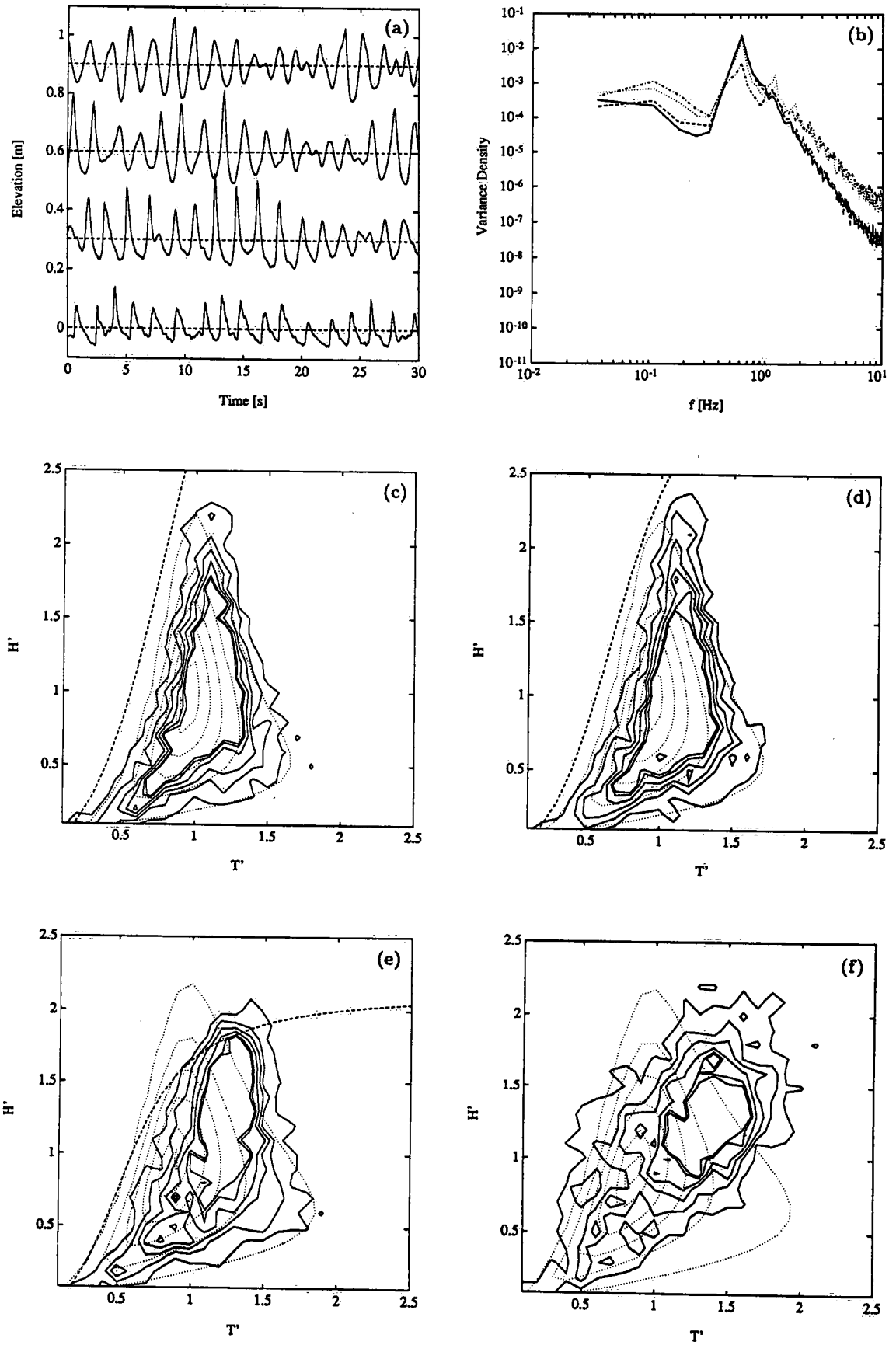

Figure 5

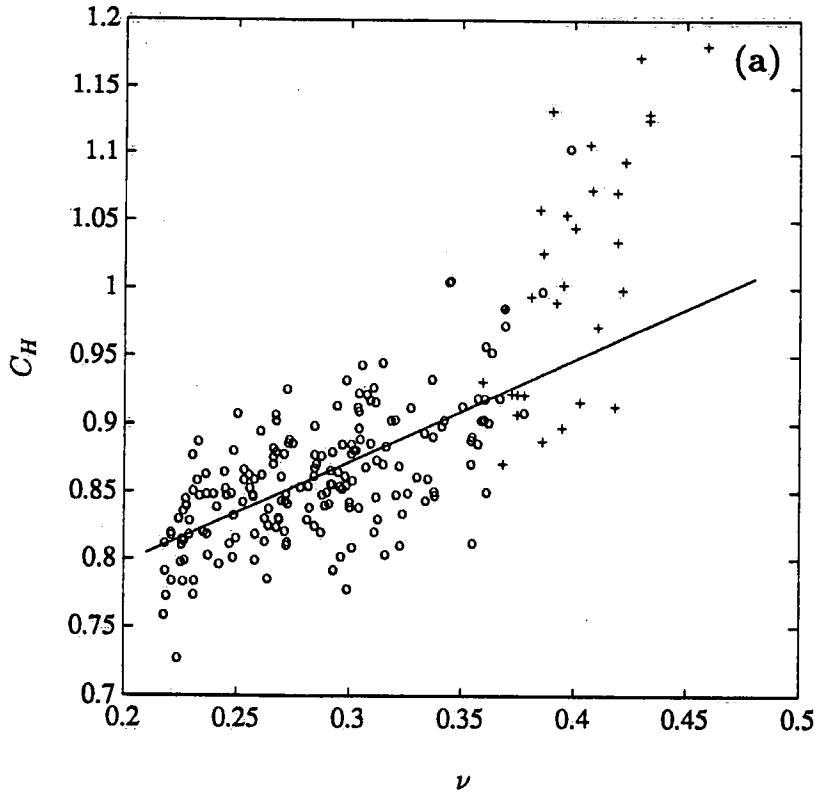
(a)
C_H
1.2
1.15
1.1
1.05
1
0.95
0.9
0.85
0.8
0.75
0.7
0.2
0.25
0.3
0.35
0.4
0.45
0.5
ν

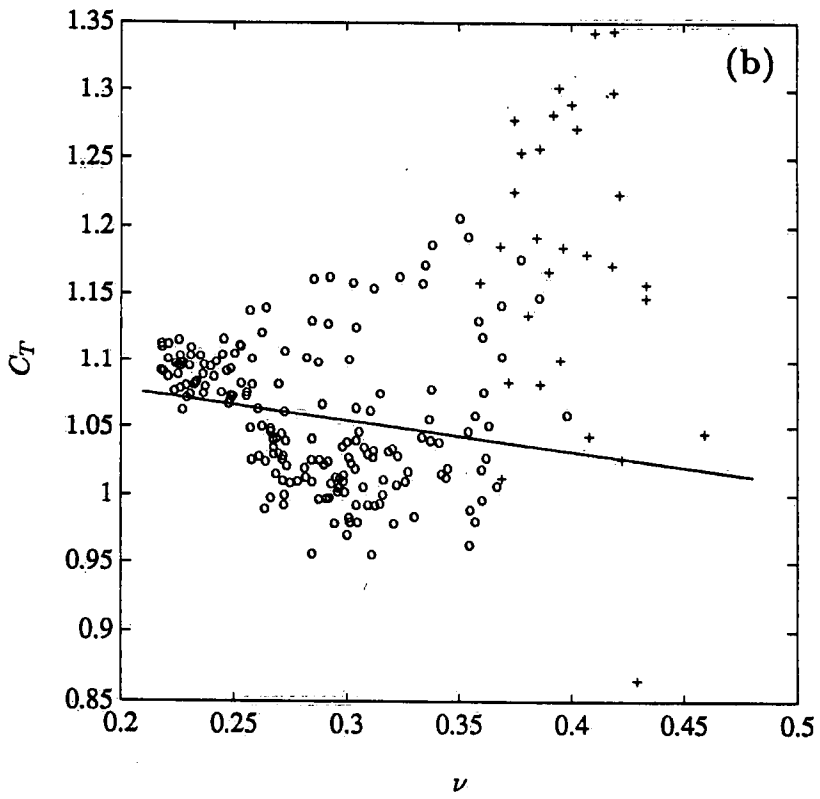
(b)
C_T
1.35
1.3
1.25
1.2
1.15
1.1
1.05
1
0.95
0.9
0.85
0.2
0.25
0.3
0.35
0.4
0.45
0.5
ν

Figure 6

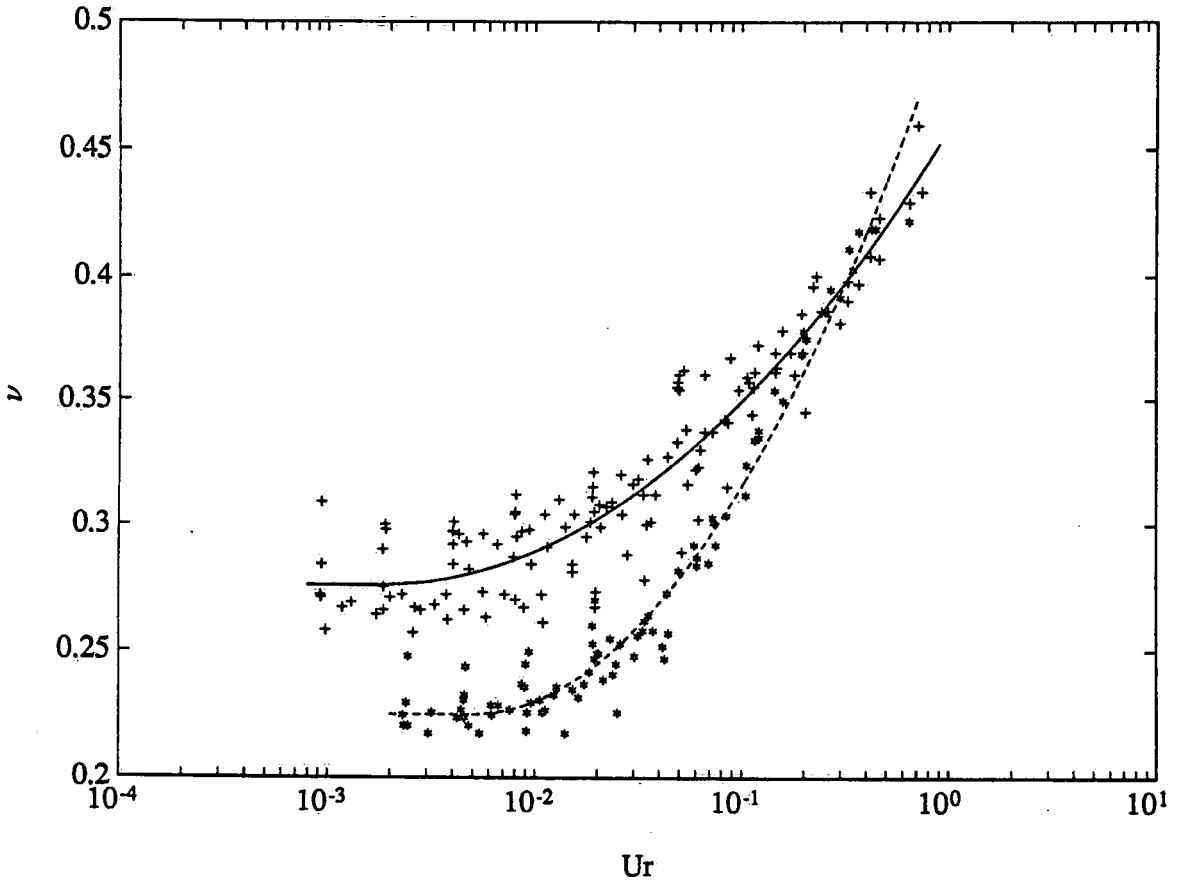

Figure 7

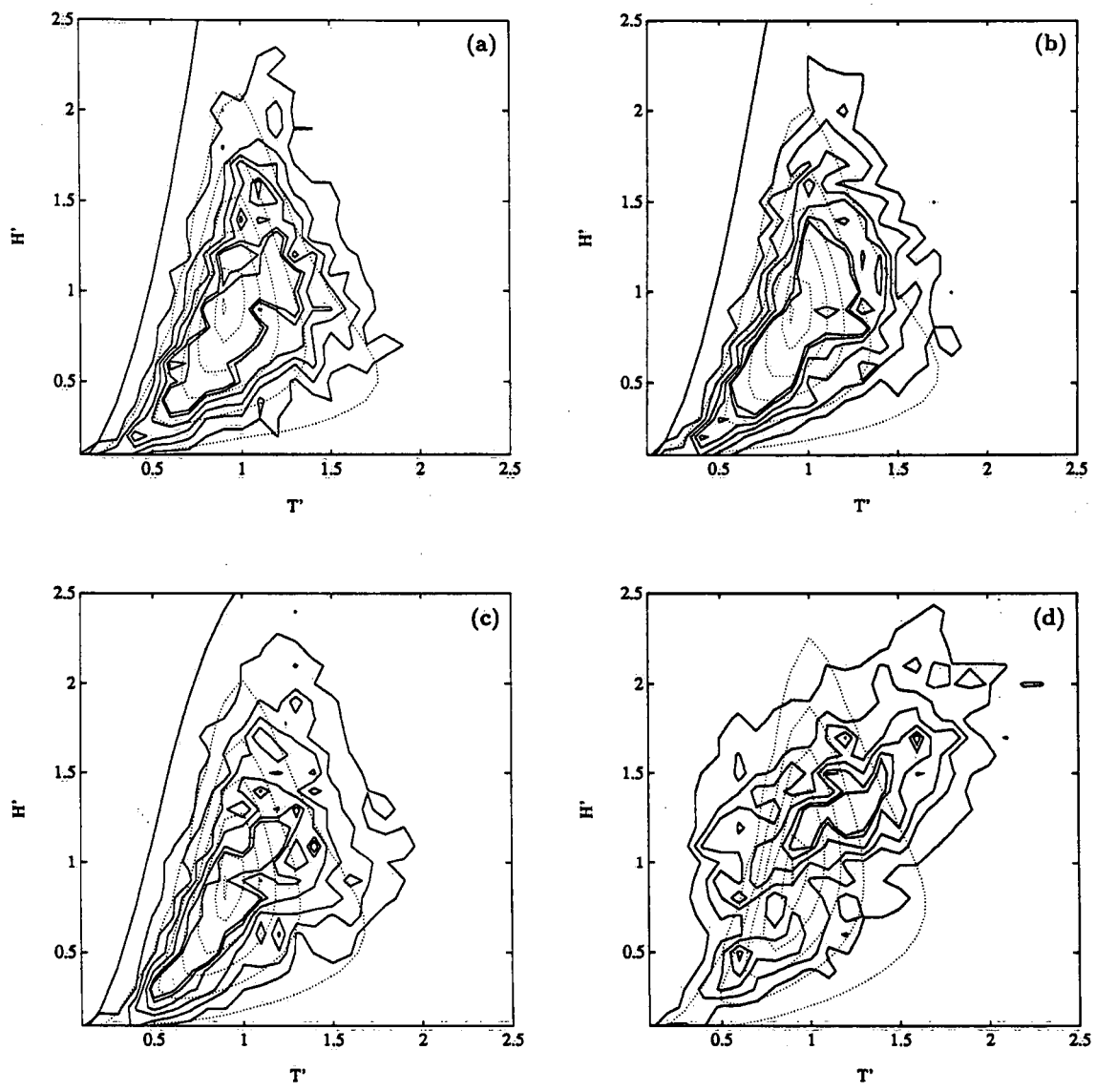

Figure 8

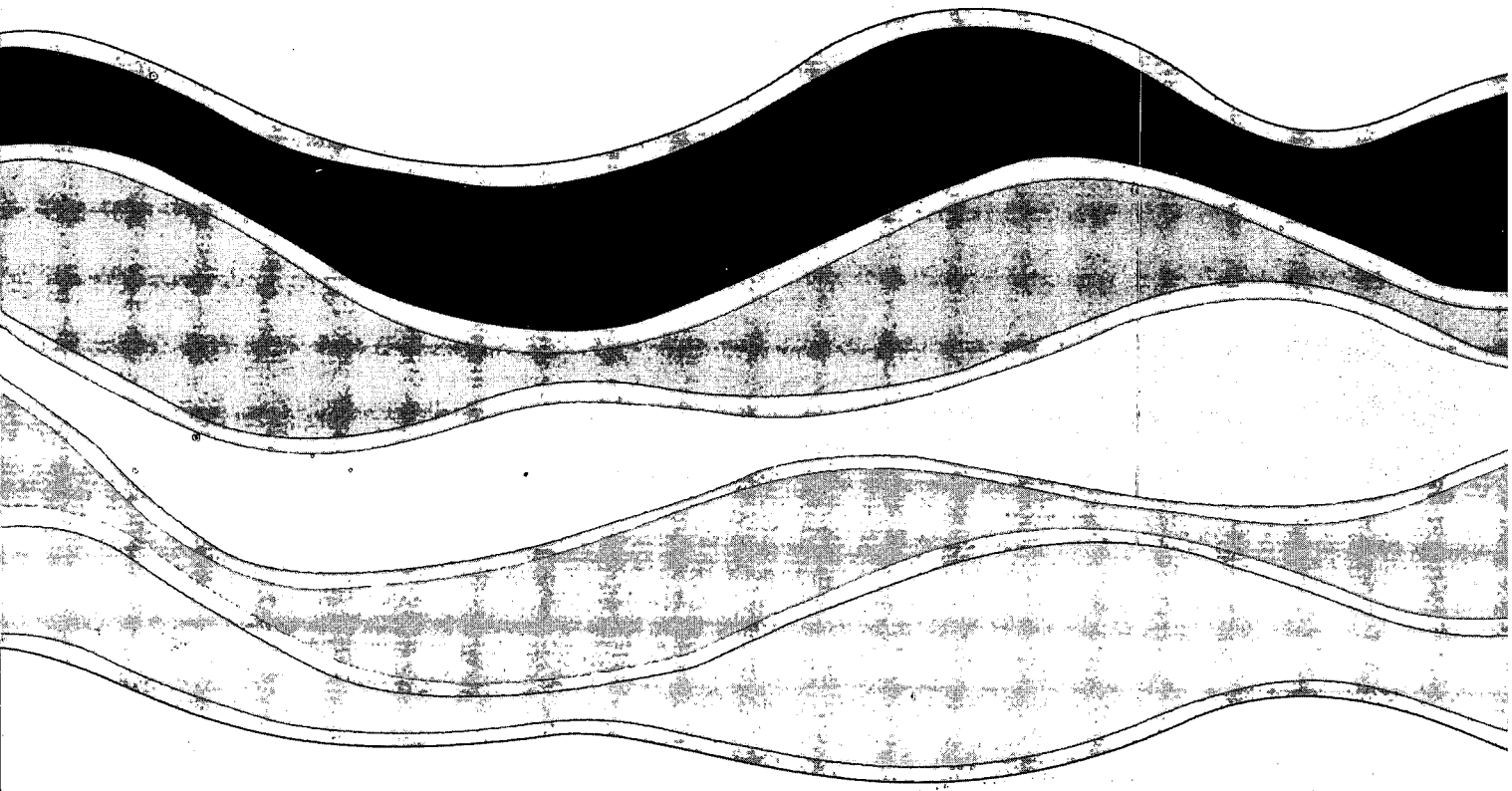

NATIONAL WATER RESEARCH INSTITUTE
P.O. BOX 5050, BURLINGTON, ONTARIO L7R 4A6

Environment Canada Environnement Canada

Canada

INSTITUT NATIONAL DE RECHERCHE SUR LES EAUX
C.P. 5050, BURLINGTON (ONTARIO) L7R 4A6

Think Recycling!

Pensez à Recycling!